

Article

Emission Factors of Tyre Wear Particles Emitted by Light Road Vehicles in Real Driving Conditions: A New Challenge for Clean Road Transport to Improve Urban Air Quality

Salah Khardi

EASE Laboratories, University Gustave Eiffel, Lyon Campus, 25 Avenue François Mitterrand, 69675 Bron, France; salah.khardi@univ-eiffel.fr

Abstract: Non-exhaust road transport emissions in cities contribute to poor air quality and have an impact on human health. This paper presents a new study of particles emitted by tyre wear in real driving conditions and gives their emission factors. The most frequently emitted particles were collected in urban, suburban and road areas. They were identified and analysed physically and chemically. Their level of toxicity is well known. An overall analysis of the measured pollutants was carried out to assess their emission factors in real driving situations. The highest emitting pollutants, considered separately, were found to have high emission factors. The values obtained exceed the Euro standard for vehicles but are below those of vehicles not equipped with particle filters. Significant test analysis confirmed that the inertia of chemical pollutants is homogeneous. Emission factors have also been provided for PM₁₀ and PM_{2.5}. These results should contribute to the emergence of future regulations of non-exhaust emissions and should help to analyse the exposure-impact relationship for particles from tyre wear.

Keywords: air pollution; emission factors; road transport; non-exhaust emissions; tyres and road dust; particle measurements; health



Citation: Khardi, S. Emission Factors of Tyre Wear Particles Emitted by Light Road Vehicles in Real Driving Conditions: A New Challenge for Clean Road Transport to Improve Urban Air Quality. *Atmosphere* **2024**, *15*, 665. <https://doi.org/10.3390/atmos15060665>

Academic Editors: Daniele Contini and Ashok Luhar

Received: 21 March 2024

Revised: 1 May 2024

Accepted: 29 May 2024

Published: 31 May 2024



Copyright: © 2024 by the author. Licensee MDPI, Basel, Switzerland. This article is an open access article distributed under the terms and conditions of the Creative Commons Attribution (CC BY) license (<https://creativecommons.org/licenses/by/4.0/>).

1. Introduction

Air pollution from road traffic is a combination of exhaust emissions (a mixture of gaseous pollutants and particles from fuel combustion and the volatilisation/degradation of lubricants at the tailpipe) and non-exhaust emissions (mechanical abrasion of brakes, tyres and road surfaces, resuspension) [1].

Deterioration of air quality in cities has become a major concern together with environmental and health impacts [2]. Many phenomena can occur during particle exhaust emissions [3]. Measuring particle emissions from tyre road wear is complex, in particular because it involves mechanical abrasion and the resuspension of particles. In fact, a non-negligible percentage of particles may be deposited. Compared to fine and ultra-fine particles, these are mainly of large size [4]. Kreider et al. [5] confirmed that the elements Ca, Fe, K, S, Zn, Mg, Al, Si, and Ti are emitted from road materials. Zinc compounds are a tyre marker [6]. Hildemann et al. [7] and Gustafsson et al. [8] cited Zn among the elemental compounds. Dahl et al. [9], Pant and Harrison [10] and Harrison et al. [11] found that tyres contain about 1% Zn as inorganic Zn such as ZnO and ZnS, and organic compounds. Belkacem et al. [1] suggested S and Zn as tyre tracers. Khardi and Bernoud-Hubac [4] and Beji et al. [12] confirmed that C, S, Cr, Cu, Ce and Zn compounds are emitted into the air by road vehicles. They confirm that Zn is a particle tracer of tyre emissions. Particle emissions are generally thermal in nature due to friction with the road surface.

Effects of particle emissions by road traffic on human health and the environment have been regularly reported [13], including cardiac system disorders, lung inflammation, asthma, chronic lung diseases, cancers and pulmonary fibrosis. Diseases are documented in the open literature; they are associated with pollutant exposure. It is confirmed that

road transport contributes to the described impacts [14]. Particles can reach the alveoli, thus causing toxic effects in the lungs [15]. Particles less than $0.5 \mu\text{m}$ enter the bronchi and lungs. Between $0.1 \mu\text{m}$ and $1 \mu\text{m}$ fine particles can therefore penetrate deep into the respiratory system. This highlights the link between the mechanical properties of the particles and the risk that they are deposited in the respiratory system. Genotoxic damage was observed [16], which can have serious health consequences [17]. Kreider et al. [18] suggested a risk assessment calculation considering exposure duration for humans.

The largest particles are stopped by inertia in the nasopharyngeal segment, but the smallest particles (less than $2 \mu\text{m}$) are also stopped by Brownian diffusion. Particles above $10 \mu\text{m}$ are stopped by the nose and do not enter the respiratory system.

This paper focuses on non-exhaust emissions by tyre road abrasion in real driving (urban, suburban, highway). Emission factors (EFs) are given using multivariate data analysis (Hierarchical Classification on Principal Components, or HCPC) to investigate pollutant identification. The method was carried out in three stages: initially, through a specification of the most predominant granulometric intervals of tyre-road emissions; secondly, an analysis of the chemical composition of the emitted pollutants and their importance; and finally, the provision of the emission factors of road-tyre pollutants supported by a solid statistical analysis.

2. Materials and Methods

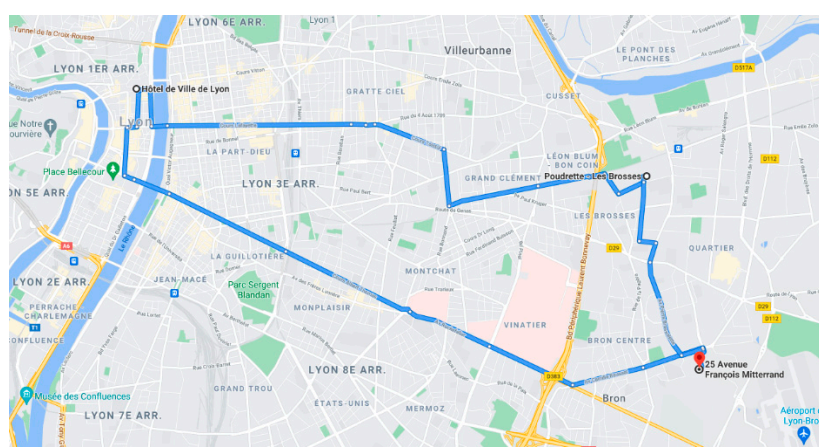
2.1. Experimental Set-Up

Experiments were carried out in the city of Lyon (France) in three experimental conditions (urban, suburban and highway) in the summer (265,760 vehicles a day) [19].

Table 1 presents measurement features (type of road, travelled distances, average meteorological conditions) during experiments in real-time driving conditions: 450 km urban, 650 km suburban and 850 km on the highway (Figure 1).

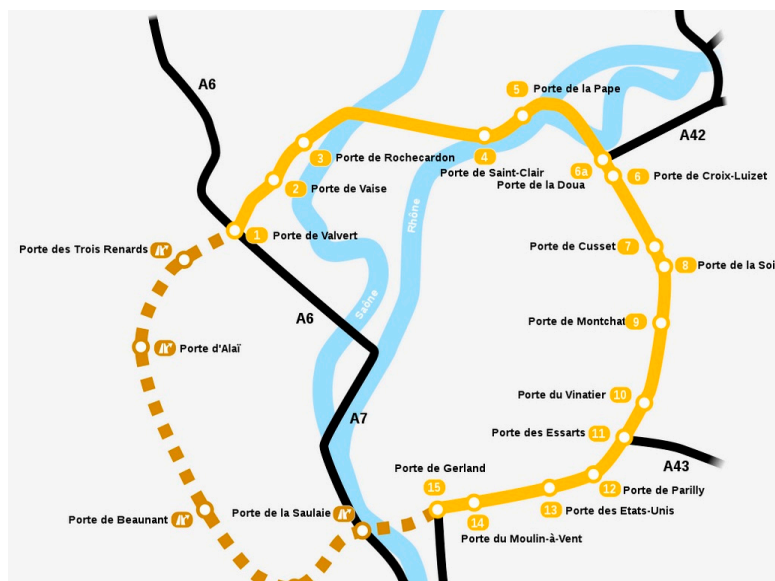
Table 1. Real driving conditions (wind speed less than 4 m/s).

Type of Route	Distance Travelled per Trip	Average Temperature (°C)	Strength of the Wind (m/s)	Relative Humidity (%)
Urban (U)	45 km	17	2	45
Suburban (SUB)	65 km	15	3	39
Highway (H)	85 km	18	2.2	53

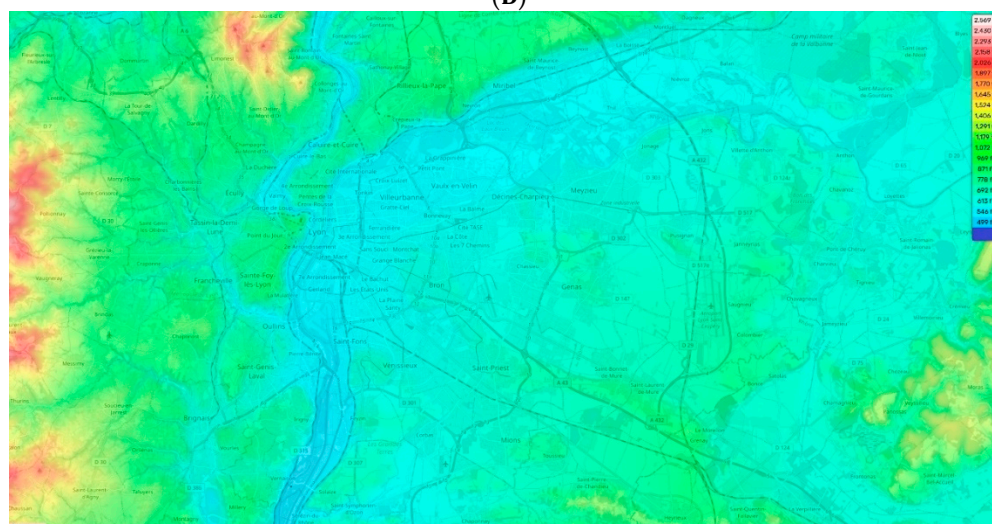


(A)

Figure 1. Cont.



(B)



(C)

Figure 1. Experimental areas (A,B) and altimetry (C) where particles were collected. (A) Urban trip (blue). (B) Suburban circuit in yellow [20]. The highway is the extension of the suburban circuit A43 (France—Source Google). (C) Altimetry of Lyon [21]. (The urban routes were in the city of Lyon and its inner suburbs, the suburban routes on the D29 and D517 departmental roads and the highway routes on the A43 motorway).

The topographical map of the city of Lyon (surface area, 47.87 km²) and its surroundings are given in Figure 1. The average altitude of the city and surrounding area is 210 m, the minimum is 161 m, and the maximum is 333 m (Altimetry of Lyon, 2023). The urban environment of Lyon presented an average road gradient of 12%, with the steepest gradient at 30%. In suburban and motorway environments, the average gradient was 3% on 70% of the experimental routes and 4.2% on the remaining 30%.

The speed of the vehicle and its position have been collected using a global positioning system under real-world monitoring with a sampling of 1 Hz (1 s⁻¹).

In this experimental work, the simultaneous measure of sizes of particles (granulometry) and their collection on carbon adhesive tabs (ϕ 47 mm) and polycarbonate Whatman[®] Nuclepore[™] Track-Etched Membranes (ϕ 25 mm) enabled the analyses of their chemical composition and identification. Membranes were considered free of traces of the chemical elements. No distinction can be made between tyre emissions and road abrasion emissions.

All measuring instruments were synchronised. An electronic device with a fixed impedance was used by injecting a square wave signal every 5 min to guarantee synchronisation between measurement systems. An optical particle counter, a GRIMM™ EDM 180 ('EDM' Environmental Dust Monitor for measuring particulate matter concentration (PM₁₀, PM_{2.5}) in ambient air) [22], was used to measure particle concentrations (ϕ [0.35 μm , 22.5 μm]) with a flow rate of 1.2 L/min and 0.1 $\mu\text{g}/\text{m}^3$. Real-time measurements in ambient air of PM₁₀, PM_{2.5} and PM₁ were carried out. This is considered an automated monitoring system using a diagnosis software system. The GRIMM™ EDM 180 was calibrated by the GRIMM Group company using dolomite dust. In comparison with other existing laboratory systems used in this research field, the GRIMM system was preferred due to its easy operability and effectiveness (i.e., small size, light weight, high battery life, low power consumption, large data storage capacity, 12 V power supply). All the used data collection systems were synchronised, allowing for good results and an explanation of the observed data. Before every measurement campaign, zero calibration was regulated on the GRIMM. During experiments, we also recorded the vehicle trajectory parameters, speed and acceleration. The temperature of brake pads was also recorded in real driving conditions. All measured signals were synchronised.

Each measurement was followed by blank tests lasting 15 min each in order to remove any impurities that may have been present in a residual way in the GRIMM pipe. Summer tyres were used to study particle emissions caused by tyres and road surface wear.

The sampling points were as follows: (1) in the middle of the wheel inter-axis, 3 cm from the road surface; and (2) behind the wheel at 2 cm from the middle of the wheel and 3 cm from the road surface. The particle collection tube had a diameter of $\frac{1}{4}$ " (6.35 mm). Figure 2 shows the experimental configuration of the light vehicle (passenger cars).

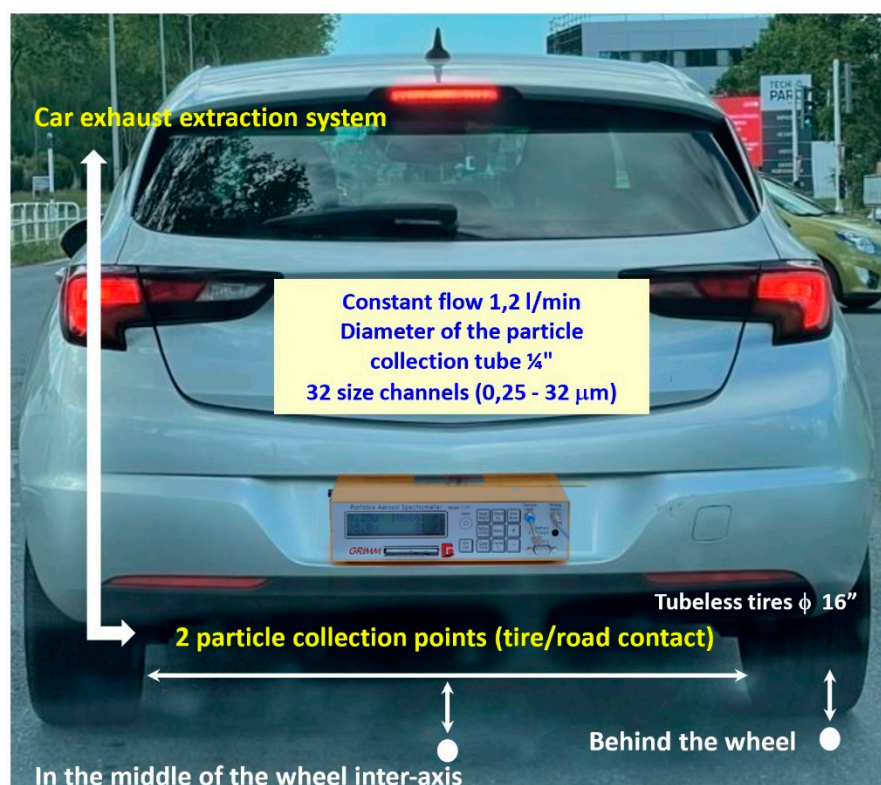


Figure 2. Two measurement points: (1) behind the wheel (2 cm from the middle of the wheel and 3 cm from the road surface); and (2) in the middle of the wheel inter-axis, 3 cm from the road surface. The particle collection tube had a diameter of $\frac{1}{4}$ " (6.35 mm). Use of Michelin summer touring tyres: 205 mm wide, 55 (height/width ratio in %), radial structure R, rim diameter 16 inches (40.64 cm).

A characterisation of the pavement was not carried out because it is complex and would require a deeper material analysis. Experiments were performed with a hot engine; the vehicle was run at a standstill for 15 min and the devices tested and calibrations performed. The experiments were then carried out in driving conditions.

The installed car exhaust extraction system was a 6 cm diameter tube attached to the exhaust pipe (20 cm length, followed by a 90° elbow and a 170 cm high tube). This configuration had the advantage of avoiding a mix of particle collection between exhaust and non-exhaust emissions. The tests were carried out on days when road traffic was very low and in off-peak hours to avoid cross-contamination from other vehicles. The collected tyre emissions from the rear axle of the vehicle were then analysed. These particle emissions are normally higher than those from the front axle of the vehicle dedicated to steering. Therefore, this experimental approach was not carried out for several reasons, namely: (1) due to experimental limitations and difficulties in collecting data related to only tyre wear; (2) in addition to collecting tyre wear particles, it collected particles originating from different sources, including exhaust, resuspension and various contaminations. The methodologic choice was to have a screen effect, which is supposed to limit the collection of all particles that would make the result interpretation complex. Thus, carbon membranes were placed on the front axles of the vehicle and analysed to control for possible contamination.

As for brake system temperature control and exhaust emissions, the control of the brake temperature was an important element in analysing the exhaust emission rate and, subsequently, the potential contamination of the collected tyre-road data. Indeed, the increase in brake friction could have had an impact in terms of contamination of measurements at the tyre-to-road contact point. This is one reason brake temperature was followed during the experiments; the latter gave information on their emission rate. A specific system to monitor these emissions was not installed but the brake temperature was controlled, and in some cases, data seemed inconsistent. To avoid possible contamination, tapered metal plates were installed on the back of the four wheels. The measured brake temperature is given as follows in Figure 3:

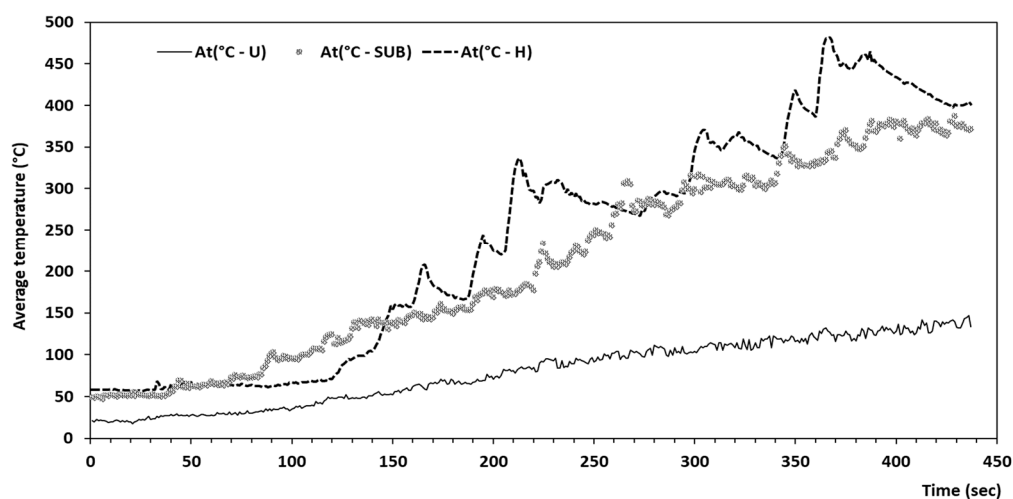


Figure 3. Control of average brake temperatures during road travels ($1\text{ }^{\circ}\text{C} = 274.15\text{ K}$).

The temperature of brakes has the advantage in tribology or contact dynamics research of offering some knowledge on the behaviour of braking systems. The measured average temperatures in urban, suburban and motorway experiments are $17\text{ }^{\circ}\text{C}$ (290 K), $47\text{ }^{\circ}\text{C}$ (320 K) and $56\text{ }^{\circ}\text{C}$ (329 K), respectively. The maximum temperatures reached are $147\text{ }^{\circ}\text{C}$ (420 K), $387\text{ }^{\circ}\text{C}$ (660 K) and $482\text{ }^{\circ}\text{C}$ (755 K), respectively. An increase in the brake's temperature occurs largely during the suburban and highway experiments (braking due to speed). With the dynamics of the vehicle in real driving conditions, no contamination of the experimental data was observed. Moreover, the results of the presented chemical analyses confirmed this. This precaution, to which was added the installation of a casing fixed on

the exhaust pipeline extending up to one metre above the roof of the vehicle, enabled the avoidance of this double contamination through brake and exhaust emissions.

The aim of this paper is to calculate emission factors for pollutants emitted by tyre and road abrasion. The experiments followed the established and known procedure from the literature. Indeed, an emission factor is applied for each vehicle category in the fleet. In the case of the experiments, it was expressed as the number of pollutants per kilometre (#/km), designating the number of pollutants emitted by the vehicle over a one-kilometre journey. It depended mainly on the vehicle type, its engine and technical features (e.g., carburation, such as petrol, diesel, LNG, and hybrid, along with cubic capacity, such as small, medium, etc.), its date of entry into service (which determines its age and therefore its wear), average vehicle speed, track gradient, average traffic speed and the proportion of the journey made with a cold engine.

The vehicle used was an OPEL ASTRA CDTI (year 2020) with the following technical specifications: fuel type, diesel; engine displacement, 1496 cm³ Inline 3; horsepower, 895 kW; maximum torque, 300 Nm; and top speed, 210 km/h.

The proportion of the experimental journey carried out with a cold engine was 2%. Of Lyon's streets, 84% are limited to 30 km/h (i.e., 610 km out of 727 km). The rest of the streets are limited to 50 km/h. Average speeds during the urban, suburban and motorway tests were 40 km/h, 80 km/h and 125 km/h, respectively. Data relating to the city of Lyon (topography, slopes, percentage of road slopes, etc.) are described above and have been represented in Figure 1.

2.2. Analysis of the Tyre-Road Surface Particles by SEM-EDX—Statistical Analysis

Analysis of the collected particles on the carbon membranes was carried out using scanning electron microscopy (SEM) associated with energy dispersive X-ray spectroscopy (EDX) [23] for identifying the elemental composition of pollutants. SEM uses an electron beam able to scan a focused stream of electrons over a given surface to produce an image with a resolution of less than 1 nm. Indeed, the electrons interact with the atoms of the sample to analyse the given signals of the chemical composition of the collected pollutants. The combination of these two techniques provided an identification of the pollutants' elemental composition. The data generated consisted of spectra showing the chemical elements collected. Thus, the energy of individual photons was measured to establish spectra representing the energy-dependent distribution of X-rays. The X-photons were captured by a solid-state detector: a lithium-doped silicon semiconductor, cooled with liquid nitrogen. X-photons cause ionisation in the semiconductor. Free electron-hole pairs migrate under the effect of the polarisation electric field and cause current pulses whose height is proportional to the energy of the photon. One can separate the impulses according to their height, and thus count the photon incidents according to their energy. This method has good sensitivity, particularly for photons with an energy between 0.2 and 20 keV. The number of photons is assessed and the count rate is expressed in count per second (cps). The main known limitation of this chemical analysis system is the width of each peak of the spectrum. Indeed, the enlargement of a peak could reflect the superposition of two or more chemical elements whose energy is close. The greater the enlargement of the peak, the more difficult the identification of a chemical element. For morphological analysis and the microanalysis of the collected dust, the use of the JSM-6510LV (JEOL Ltd.) was privileged, as it is a high-performance SEM for fast characterisation of chemical elements (low vacuum SEM, high resolution of 3.0 nm at 30 kV and good performance for pollutant identification).

The JSM was coupled to an EDX spectrometer (Oxford Aztec-DDI X MAXN 50, JEOL [24]). SEM analyses were performed at different magnifications and provided specific information on the composition of the particles. The analyses of the particles gave a comparison of their EDX spectra: retro-scattered electrons; intensity varying between 20 kV and 30 kV (high resolution of 3.0 nm at 30 kV); working distance equal to 12 mm (accelerating voltage 500 V–30 kV); variation of pressure (10–270 kg.m⁻¹.s⁻²); and magnification

($\times 5 - 300,000$). The resolution is much higher compared to that of optical microscopes, with a greater focal depth.

The fully automated INCA software (INCA: Integrated Calibration and Application Tool developed by ETAS Company) was used to analyse the collected particles. The surfaces analysed for the pollutant chemical identification were all equivalent and were of the order of 24 mm^2 . INCA offered a wide variety of efficient and fast functions to analyse data [25]. The combined system used a motorised turntable that enabled automatic analysis of 1000 particles for each sample. In addition to the INCA software, the HCPC method was used. This method was favoured over other simple classical methods that exist in the literature, such as Student's t test. It is based on numerical data classification methods [26] with a simplified application framework. Indeed, it is complete and efficient and provides excellent quality results. This method used the following processes:

- Identifying particle size ranges and groups.
- Selecting predominance sizes. This step assumes, a priori, that the sets of the same identified particles are homogeneous.
- Starting calculations and then constructing sets of particles.
- Building granulometric intervals and chemical element sets, having no consequences on the relative loss of inertia of the used calculation algorithm.

The last processing step checks error propagation and provides means, min, gravity centres, etc.

Data were processed with R software 2.1 [27], which is a free and open software environment for statistical computing. It compiles and runs on a wide variety of platforms. It is a language of programming. The processing of data with R followed numerical known steps [28–31]:

- Importing data—building the hierarchical clustering algorithm.
- Identifying chemical elements inside the same set. This step required the separation of experimental data on separate homogeneous sets of particles having equal variance that could minimise inertia in each set of data. This allowed the division of each set of data into three data sets (urban, suburban and highway), with the advantage of giving centroids of sets that measured how coherence was inside each set of identified particles.
- Choosing the number of sets of identified particles that seemed relevant based on data measurements.
- Using the principal component analysis of the FactoMineR package.
- Interpreting each chemical element.

Experiments in real driving conditions were carried out by the same driver and in the same atmospheric conditions, allowing complete synthetic results without statistical bias and confirming and appreciating the quality of the homogenisation step previously described. These analysis data exclude braking emissions; experiments were carried out in such a way that the particles emitted by the brakes were not recorded and did not impact whatsoever. Particles were classified in a family according to their chemical composition and the result is given in the form of a spectrum. As previously described, the energy of individual photons is measured to establish spectra representing the energy-dependent distribution of X-rays.

The two concrete examples of spectra given below (Figure 4) were obtained by SEM-EDX. They show a multitude of chemical elements identified with a net predominance of Si, Al, Ca, Mg, Fe and their components.

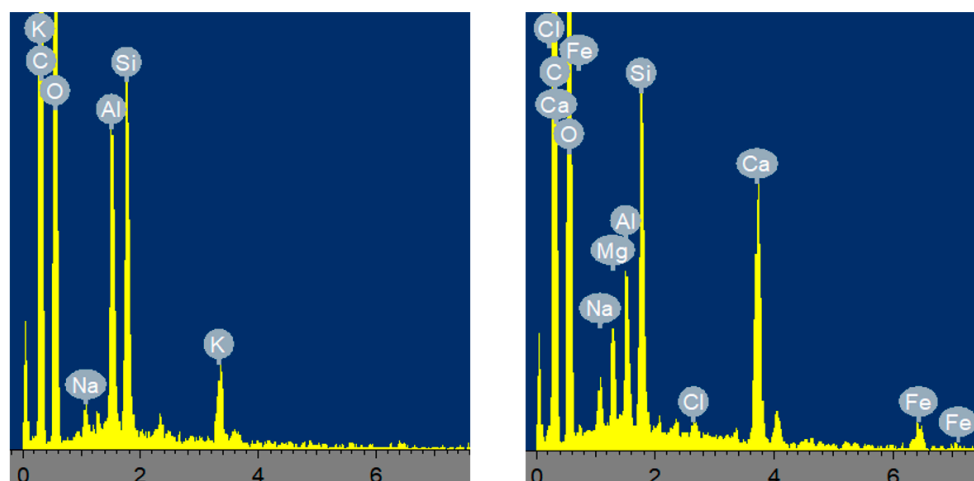


Figure 4. Example of two SEM-EDX spectra of particles (in Arbitrary Unit—Full scale 2054 cps).

In the spectra of the particles, different peaks corresponding to C, O, Al, Si, Na, Al, Si, K, Fe, Ca, Mg, Na and Cl and traces are present. This analysis was conducted spectrum by spectrum to identify all the particles present on about a hundred sample membranes. The different sets of particles obtained during this analysis were aluminosilicate, iron and silicon compounds, iron and calcium oxides, calcium compounds, silicate without aluminium, calcium phosphate, titanium and copper compounds, chromium, sulphur and barium compounds, aluminium oxide, zirconium compound and aluminium compounds, tungsten, etc., and chemical traces. Multi-elemental particles could be found in each set of compounds, with the identification of more than 33% of the total mass in the chemical element. If several elements had a mass of more than 3% of the same set of particles, the heaviest element was considered and a new set of elements was created. Finally, statistical analysis of the obtained and identified particle was carried out with R statistical software (FactoMineR package).

This paper uses the identified chemical elements by SEM-EDX. Particles considered as contaminations were eliminated. In fact, this work draws on much of the open literature that has already provided information on the wide variety of pollutants considered to be contaminants in this particular case. Larger particles are deposited on a variety of substrates (buildings, infrastructures, roads, etc.). Finer particles can be deposited by Brownian agitation. When there is any topography of the area in which particles are emitted, such as a street or neighbourhood, those with a mass greater than the gas molecules do not follow airflow, which is responsible for transport or dispersion phenomena. They continue moving in the direction in which they were originally emitted. The inertia of particles allowed them to collide or stick to obstacles in the flow. The higher the flow velocity, the greater the mass of the particles. In particular, this phenomenon concerns particles with a diameter greater than 1 μm . For example, this inertia is commonly used to separate particles according to their size in cascade impactors or cyclones. Chemical species 'i' were assessed in samples. Calculating the v_{test} [32] for species 'i' allowed us to verify the homogeneity of particles belonging to the same group. These sets consist of chemical elements with the same properties or the same chemical identification obtained by a count:

$$v_{\text{test}}[i] = \sqrt{N_{[U]}} \times \frac{f_{i/[I]} - f_{[U]}}{\sqrt{\frac{N_{i/[I]} - N_{[U]}}{N_{i/[I]} - 1} \times f_{[U]} \times (1 - f_{[U]})}}$$

where:

- i : pollutant)
- $f_{i/[I]}$: frequency of the 'i' pollutant in the group I

- $f_{[U]}$: frequency of the 'i' pollutant in all groups of data
- $N_{i/[I]}$: the relative number of 'i' pollutants in group I (having the same size)
- $N_{[U]}$: the relative number of 'i' pollutants in all groups of data I versus the total size of the groups

I is the set of identical chemical species, identified by SEM-EDX, analysed for a given surface of the sampling membrane. This surface may correspond to the total surface of the membrane if the analysis is performed on a single membrane. In this particular case, the MEB analysis surface was defined for all the particle collection membranes.

The v_test is very sensitive to the identification of pollutants by their chemical groups.

3. Results

Individual particle SEM-EDX and global analyses (granulometry—particle size) were performed, as well as the calculation of the overall values for the data obtained through SEM-EDX, in order to make comparisons. Thus, Figure 5 presents the variations of the mean values of the particle number according to the analysis by SEM-EDX of the collected particles on the membranes, and by the particle size analyser (PSA) vs. the vehicle speed. This analysis was conducted for the three types of trips: six urban trips, two suburban trips and three highway trips. The respective speed values for the three routes in France (45 km/h, 90 km/h and 130 km/h) represent the maximum values to be performed per site.

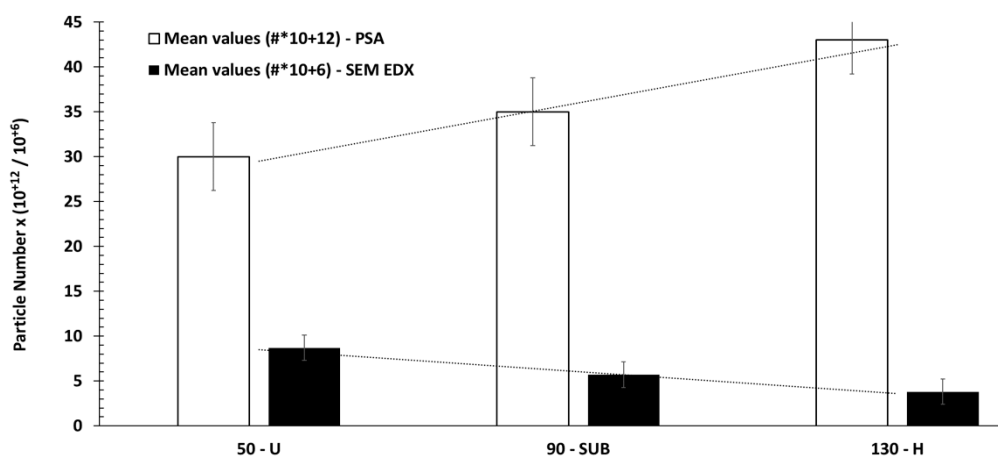


Figure 5. Number of particles depending on the type of analysis (PSA and SEM-EDX) and road (urban, suburban and motorway, respectively, with speed limits of 45 km/h, 90 km/h and 130 km/h).

It should be remembered that tyre wear particulate emissions strongly depend on the speed of the vehicle and the wear and age of the tyres, but also on the characteristics of the pavement (roughness, ageing, etc.). This work does not integrate the characteristics of the pavement because it would require the development of a consistent method, and this does not exist yet. Doing so would imply research work focused primarily on the materials that constitute the pavement, and on the online monitoring of the pavement's features; however, online monitoring of the characteristics of the pavement is almost impossible to achieve.

Figure 5 shows that there is an effect of the vehicle speed. The number of particles emitted increases with speed when measurements are made with a particle size analyser. A slight inverse effect occurred when the analysis was performed with SEM-EDX. This behaviour in the number evolution is normal and is due to the fact that a chosen surface was targeted for EDX SEM analysis. The measured average particle number values are:

- Particle size analyser: (30, 35, 43) 10^{+12} particles.
- SEM-EDX: (8.7, 5.7, 3.8) 10^{+6} particles.

The ratios (particle size count/SEM-EDX count) are $6.4 \cdot 10^{+6}$, $6.2 \cdot 10^{+6}$ and $11.3 \cdot 10^{+6}$, respectively, for urban, suburban and highway trips.

The following analysis will make it possible to extrapolate this number of particles for the surrounding particles collected throughout the membrane.

Several observations can be noted:

1. A high factor of more than 10^{+6} is found between the particle size values and the assessment of the total number of particles from the SEM-EDX results. This seems natural because the collection on the membranes is purely qualitative and serves more for chemical identification.
2. Despite uncertainties in both particle size counts, there is an inversion of the curves between particle size and chemical particle count as a function of velocity. On the one hand, considering the SEM-EDX count, more particles were collected in the urban area than on highways because of the vehicle speed. This is certainly due to the dynamics of emissions as a function. On the other hand, the inversion of this curve, obtained by the particles collected by the granulometry method, seems in favour of the speed. The faster we drive, the more we collect. This figure confirms that the physicochemistry is preserved with this double collection independently of the variations that can be observed. Therefore, precaution must be taken when counting particles from the collection on membranes for chemical analyses. In this case, the emission dynamics, which are a function of the speed of the vehicle, could not be confirmed.

In conclusion, the SEM-EDX count is qualitative in favour of the chemical identification of emitted particles. On the other hand, the particle size count is quantitative. Based on the collection of particle size data, the analysis of the most emissive particle size intervals is shown in Table 2 in order of importance in terms of emission:

Table 2. Predominance order of the collected particle sizes (U, SUB, H).

Predominance Order of Particle Sizes	U	SUB	H
1st class	<1 μm	<1 μm	<1 μm
2nd class	1–2 μm	1–2 μm	1–2 μm
3rd class	-	2–3 μm	2–3 μm
4th class	-	-	3–4 μm

We can observe in this table that the grain size range widens from the urban to the motorway emissions. Particles less than 1 μm are the most present in the three road routes, followed by the interval 1 μm and 2 μm , and finally 2 μm and 3 μm for suburban and 3 μm and 4 μm for highway. The synthesis thus provides a general predominance of particles emitted in the particle size ranges of [$<1 \mu\text{m}$, 2 μm], [$<1 \mu\text{m}$, 3 μm] and [$<1 \mu\text{m}$, 4 μm], respectively, for urban, suburban and highway experiments.

The percentages of the predominant particle size classes are 72.7% for the first two combined classes, 21% for the third and 6.3% for the fourth. The effect of the speed of the vehicle, and therefore the potential for collecting particles online, is certainly obvious. These percentages are therefore consistent with what was observed in the literature [1,4,33]. The first two particle size classes are known to have the highest degree of toxicity [34] because they easily penetrate the lungs and cross biological barriers to reach vital organs, which may cause significant health consequences.

Number concentrations are therefore dominated by particles $<1 \mu\text{m}$, while most of the mass was in particles $>1 \mu\text{m}$. This result agrees with the work of Alves et al. [35]. These authors found mostly 0.5 μm instead of 1 μm , which is not really in contradiction with this result if it is refined further; thus, further refinement would not be necessary because it does not improve the results.

In general, the obtained results of our experiments complete those found in the open literature, in particular those of Beji et al. [2], Harrison et al. [13], Sadiq et al. [11], Piscitello et al. [33], Andrea et al. [34], Alves et al. [35] and Zhang et al. [36].

Analysing the particle number collected by the analyser allowed us to calculate the emission factor for four different situations: (1) on an urban site where the traffic speed is between 30 and 50 km/h; (2) on a suburban site where the speed limit is 90 km/h; (3) on a highway where the speed limit is 130 km/h; and (4) in a traffic zone on an urban site in the city. Granulometric data was collected with ATMO AURA fixed systems. Among the data collected, the following selection was made: six urban (U1 to U6), two suburban (SUB1 and SUB2) and three highway (H1 to H3) routes. For comparison, the collection then analyses a series of data recorded during four days corresponding to a static urban traffic site (S1 to S4). The data were collected during days when the weather conditions were identical to the other experiments (U, SUB, H).

Figure 6 shows emission factors (EFs) in the number of particles per km travelled (#/km).

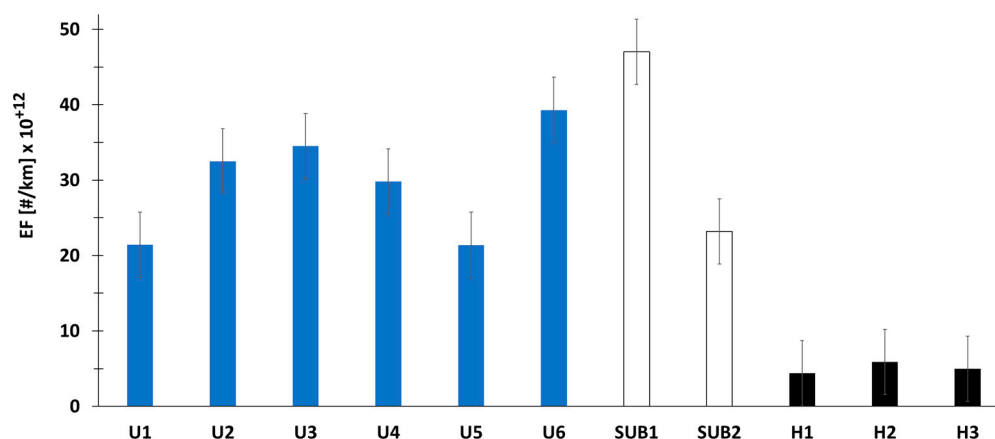


Figure 6. Emission factors for three different driving situations. Maximum authorised speed [Urban ‘U’ (50 km/h)—Suburban ‘SUB’ (90 km/h)—Highway ‘H’ (130 km/h)].

The emission factors are of the order of $30 \times 10^{+12} \#/km$ and $35 \times 10^{+12} \#/km$ for urban and suburban, respectively. We observe that there is a difference between urban and peri-urban of $5 \times 10^{+12} \#/km$. However, on highways, the emission factor, on average in the order of $5 \times 10^{+12} \#/km$, is much lower than the two previous situations. The emission factor obtained on the highway trip is of the same order of magnitude as the difference between urban routes and suburban driving situations. The number of particles was calculated for a duration equal to the duration of urban experiments U1 to U6. Finally, for the urban traffic situation site, we have, on average, a number equal to $43 \times 10^{+12} \#/cm^3$ (S). This value (number of particles per unit volume) cannot be related to an emission factor obtained in real driving conditions. However, this higher value, in a static urban site, can be considered quite high. This is due to the accumulation of pollutants in a fixed urban site, corresponding to the ambient air pollution in this urban point location.

The obtained EFs for the three types of experiments are above the value of the Euro 6 standard (fixed at $6 \times 10^{+11} \#/km$) for both diesel and petrol vehicles. It can also be noted that these EFs are below the values corresponding to diesel vehicles not equipped with particle filters ($6 \times 10^{+13} \#/km$), where the ratios are 2 (U), 1.7 (SUB), 12 (H) and 1.4 (S). As a reminder, the New European Driving Cycle gives a limit value of $6 \times 10^{+11} \#/km$ (Euro 6b) for PN (number of particles per km) for spark-ignition engines (gasoline, LPG, etc.), including hybrids, and a limit value of $6 \times 10^{+12} \#/km$ for diesel engines only, including hybrids. In the future, we shall be seeing stricter regulations on the limit values.

It can be noted that the number of particles is quite similar in the city static situation compared to experiments performed in real driving conditions. This is due both to the dispersion of pollutants but also to the effect of accumulation in a localised static point. Figure 7 shows the number of particles per cm^3 at this static point in the urban area of Lyon. For all the performed experimental measurements, with uncertainties, the number

of particles per cm^3 is greater in a static situation in a city ($\approx 42.8 \cdot 10^{12} \text{ \#/cm}^3$) than in a real driving situation (approximately $30 \cdot 10^{12} \text{ \#/cm}^3$ in urban and $35.1 \cdot 10^{12} \text{ \#/cm}^3$ in suburban). This is due both to the dispersion of pollutants and the effect of accumulation in a localised unpoint.

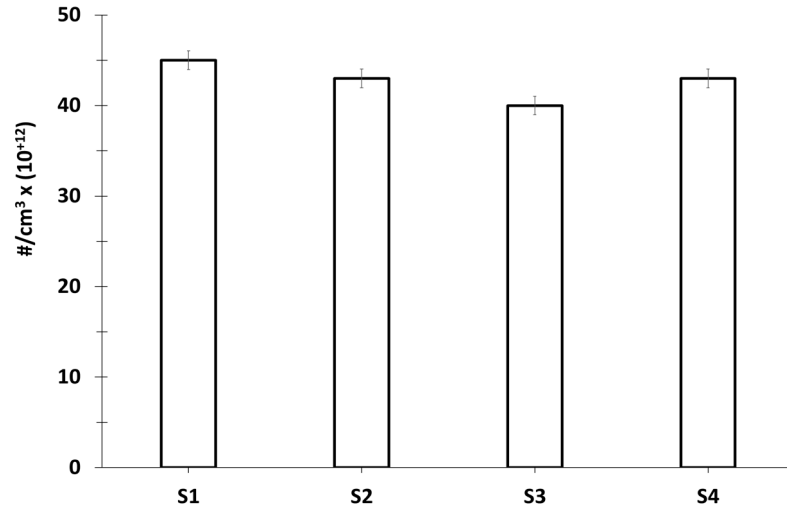


Figure 7. Evaluation of the average number of particles per cm^3 in the traffic site, at a fixed location in an urban environment (S1—S2—S3—S4).

These results allowed us to evaluate the average corrective factor (ACF) between the analysis of emission factors obtained by particle size analysis and those obtained by identification using SEM-EDX. These average factors are $3.4 \cdot 10^6$ (urban), $6.1 \cdot 10^6$ (suburban) and $11.3 \cdot 10^6$ (highway), respectively.

Thus, the number of particles used in the chemical identification of pollutants, obtained by SEM-EDX analysis, is multiplied by this corrective factor to obtain the number of particles that would be analysed online in real driving situations. This analysis enabled to establish the emission factors by chemical element as presented in Figure 8, which shows the average emission factors (EFs) for the 19 identified pollutants.

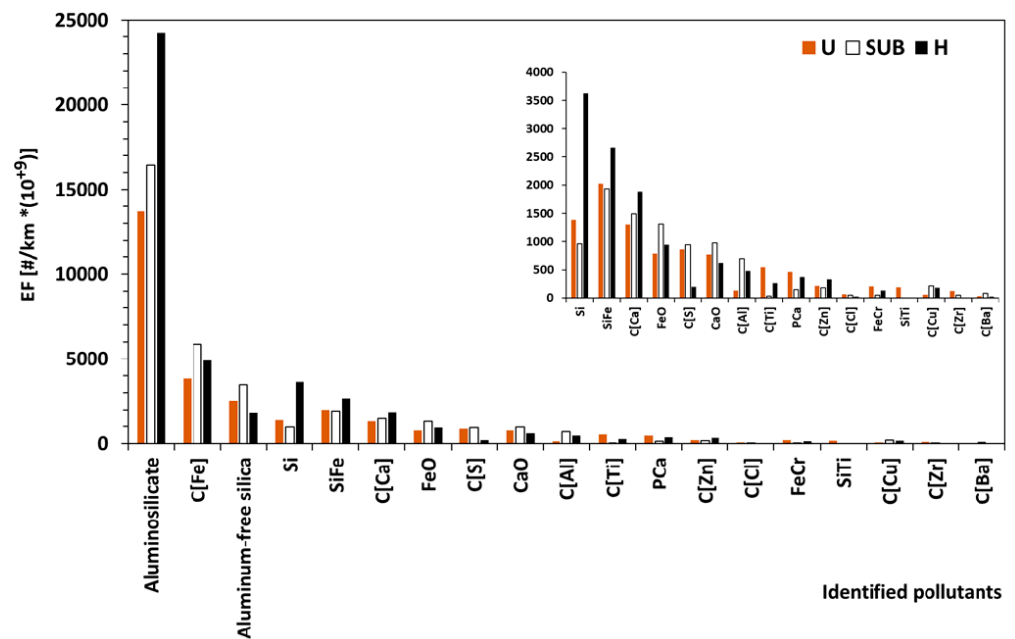


Figure 8. Emission Factors for the identified individual pollutants in real driving.

We note the predominance of aluminosilicate, Fe components, aluminium free of silica, Si, SiFe, Ca components, and FeO. For the rest of the pollutants, the A_EFs are low. This does not mean that they should not be taken into account in any environmental or health impact analysis, as this will naturally depend on the volume of the vehicle fleet.

Table 3 gives the emission factors for 19 pollutants identified using the SEM-EDX technique. These are emission factors obtained experimentally in the region closest to their emission sources (tyres—road surface). In the analysis of pollutants taken individually, the EF ranges from 0.003 to $18.142 \cdot 10^{+12}$ #/km.

Table 3. Emission factor for 19 individual pollutants.

	Identified Pollutants by SEM-EDX	Emission Factor [#/km * 10^{+9}]	Percentages (Compared to the Total Number)
1	Aluminosilicate	$18,142 \pm 597$	50.9%
2	C[Fe]	4881 ± 175	13.7%
3	Aluminium -free silica	2612 ± 57	7.3%
4	SiFe	2206 ± 60	6.2%
5	Si	1989 ± 36	5.6%
6	C[Ca]	1558 ± 32	4.4%
7	FeO	1013 ± 33	2.8%
8	CaO	789 ± 26	2.2%
9	C[S]	667 ± 25	1.9%
10	C[Al]	436 ± 27	1.2%
11	PCa	329 ± 17	0.9%
12	C[Ti]	281 ± 11	0.8%
13	C[Zn]	240 ± 8	0.7%
14	C[Cu]	152 ± 5	0.4%
15	FeCr	129 ± 9	0.4%
16	SiTi	64 ± 7	0.2%
17	C[Zr]	58 ± 9	0.2%
18	C[Ba]	46 ± 11	0.1%
19	C[Cl]	39 ± 11	0.1%

By way of comparison, the Euro 6 standard is set at $6 \cdot 10^{+11}$ #/km for both diesel and gasoline. For diesel vehicles not fitted with a filter, the given value is $6 \cdot 10^{+13}$.

Experiments do not take into account a heterogeneous mixture of components from P, Cl, Fe, Ba, Cr, or Zr that represent a percentage of less than 0.1% of the total number of particles identified. The application of Pearson and Spearman tests [37] showed that correlations were significant, with $p < 0.02$. In addition, analysis of the inertia of chemical species has been carried out to confirm the homogeneity of their identification.

A v_{test} is equal to 1.92 for urban pollutants, 1.97 for suburban, and -1.87 for highway ($p \cong 5\%$). The chemical inertia of pollutants was found to be consistent, and data analysis was significant ($v_{\text{test}} \cong \pm 2$). This finding provides additional information to the work by Belkacem et al. [1], Piscitello et al. [33], Zhang et al. [37] and Kaul and Sharma [38]. Furthermore, Piscitello et al. [33] gave emission factors as follows: 0.3 mg/km to 7.4 mg/km for tyre wear, and 5.4 mg/km to 330 mg/km for resuspended dust.

Finally, an attempt was made to approximate the EF of the PM_{10} and $PM_{2.5}$ from the calculations by Zhang et al. [37]. Indeed, by assessing the density of those two major air pollution determinants, with a conversion of the number into mass and assuming that

all the particles are identical and spherical, the obtained EF is 1.45 mg/km for PM₁₀ and 0.35 mg/km for PM_{2.5}. These EF values are close to those obtained by Zhang et al. [36] (0.21 mg/km for PM_{2.5} and 1.27 mg/km for PM₁₀), who carried out experiments on a tyre dynamometer. The small difference can be attributed to the fact that this new additional work assesses all the emissions from tyre road surface wear and not the emissions from the tyre alone.

This shows that the new methodological approach used in this paper is particularly effective in assessing pollutant emission factors. It is a new alternative to existing methods that are sometimes very difficult and costly to implement. In addition, Alves et al. [35] generated wear particles on a road simulator to study the interactions between tyres and a composite road surface. They found that the emission factor due to wear between their particular road surface and the tyres was of the order of 2 mg/km. On the one hand, work carried out on any simulator under controlled conditions often deviates from reality or actual vehicle use. On the other hand, this estimate is not very far removed from the new results being produced and obtained with experiments carried out in real driving situations.

4. Conclusions

This paper presents a reliable method combining the collection of particle emissions by tyre road surface wear in real driving on urban, suburban and highway routes. Comparatively, the data was collected on a site located in the city, on a boulevard where traffic is very important. The objectives of this significant experimental work were achieved, providing the most predominant pollutant emission factors using a robust and effective experimental approach. To determine the chemical compositions and then emission factors of particles emitted by tyre road surface wear without contamination from brake dust, measurements were performed in real driving conditions. SEM-EDX has been used to identify the measured chemical elements and their nature. Predominant particles emitted by tyre road surfaces have been analysed and emission factors for 19 identified pollutants assessed for the first time using this new approach. The significant findings include:

1. The mainly most measured tyre road surface particles were smaller than 1 µm for the three road routes, followed by particles of interval size [1 µm, 2 µm]. Then, in the third position, we have the size range [2 µm, 3 µm] for suburban and highway; and in the fourth position, the range [3 µm, 4 µm] for highway alone. It should be noted that particles of between 2 and 4 µm are emitted in urban and between 3 and 4 µm in suburban experiments, but at low proportions due to emission dynamics (vehicle-tyre-pavement) related to the movement of the vehicle and the tribology of the materials that constitute the tyres and the road surface.
2. The collected data showed a large variety of chemical elements emitted in real driving. The systematic presence of carbon and oxygen was noticed.
3. Emission factors (EFs) were calculated on the basis of granulometric and global chemical analysis of the measured data: the average values for all measured pollutants are $30 \cdot 10^{+12}$ #/km and $35 \cdot 10^{+12}$ #/km, respectively, for urban and suburban. However, on the highway, the EF is equal to $5 \cdot 10^{+12}$ #/km, about 6 to 7 times lower than the previous two. In the analysis for pollutants taken individually, the EF ranges from 0.003 to $18.142 \cdot 10^{+12}$ #/km. Significance test analysis was carried out for the identified pollutants and their EF. A *v*-test was found to vary between 1.87 and 1.97 (*p* ≅ 5%). The inertia of chemical pollutants was found to be homogeneous, and analysis is therefore considered reliable, with a *v*-test ≅ ±2.
4. The obtained EFs are above the value of the Euro 6 standard of $6 \cdot 10^{+11}$ #/km for both diesel and petrol vehicles. The EFs are below the values corresponding to diesel vehicles not equipped with a particulate filter ($6 \cdot 10^{+13}$ #/km). As a reminder, the New European Driving Cycle gives a limit value of $6 \cdot 10^{+11}$ #/km (Euro 6b) for PN (number of particles per km) for spark-ignition engines (gasoline, LPG, etc.), including hybrids, and a limit value of $6 \cdot 10^{+12}$ #/km for diesel engines only, including hybrids.

5. The assessments of EF of the PM₁₀ and PM_{2.5} emitted by the tyre road surface wear are 1.45 mg/km and 0.35 mg/km, respectively.
6. The particle number per volume element in a static situation in the city is $\approx 42.8 \cdot 10^{12} \text{ \#/cm}^3$. This number of particles is stable almost every day, except in summer holiday periods and Sundays, when urban traffic is low in the city. In real driving situations, we obtained $30 \cdot 10^{12} \text{ \#/cm}^3$ in urban and $35 \cdot 10^{12} \text{ \#/cm}^3$ in suburban. The larger measured number on the fixed site is due both to the dispersion of pollutants and to the effect of accumulation in a localised unpoint.

These results show that the methodological approach used in this paper is particularly effective in assessing pollutant emission factors. This kind of approach is a new alternative to existing methods. The significant obtained results in this paper thus provide reliable information to help improve emission models, making them more accurate and applicable. Further research integrating the phenomena of resuspension of particles in the air is necessary. These researchers will bring other scientific knowledge to the work presented in this paper. They will have to consider the nature of the materials of the road surfaces and tyres, whose physicochemical characteristics must therefore be specified. Thus, methods must be developed to separate the particles emitted by tyres and the road surface. These particles will have to be analysed individually and, if possible, online, to avoid chemical transformations that induce secondary pollution, because airborne particles can differ significantly from friction materials. Then, experimental conditions will have to be controlled and, if necessary, supported by new tool developments. The problem could become insoluble if we do not take into account the complex mixing effect between exhaust and non-exhaust emissions.

The results presented in this paper will contribute to future regulations for road vehicles (thermal, hybrid, electric, autonomous). Further scientific work, such as analysing exposure-impact relationships to TRWP, is needed to complete the development of technical and legislative recommendations, as well as health guidelines.

Funding: This research received no external funding.

Institutional Review Board Statement: Not applicable.

Informed Consent Statement: Not applicable.

Data Availability Statement: The data presented in this study are available on request from the corresponding author due to privacy reasons.

Conflicts of Interest: The authors declare no conflict of interest.

References

1. Belkacem, I.; Khardi, S.; Helali, A.; Slimi, K.; Serindat, S. The influence of urban road traffic on nanoparticles: Roadside measurements. *Atmos. Environ.* **2020**, *242*, 117786. [[CrossRef](#)]
2. Beji, A.; Deboudt, K.; Khardi, S.; Muresan, B.; Lumiere, L. Determinants of rear-of-wheel and tire-road wear particle emissions by light-duty vehicles using on-road and test track experiments. *Atmos. Pollut. Res.* **2021**, *12*, 278–291. [[CrossRef](#)]
3. Milojević, S.; Glišović, J.; Savić, S.; Bošković, G.; Bukvić, M.; Stojanović, B. Particulate Matter Emission and Air Pollution Reduction by Applying Variable Systems in Tribologically Optimized Diesel Engines for Vehicles in Road Traffic. *Atmosphere* **2024**, *15*, 184. [[CrossRef](#)]
4. Khardi, S.; Bernoud-Hubac, N. Pollutant Emissions of Vehicle Tires and Pavement in Real Driving Conditions. *J. Environ. Pollut. Control* **2022**, *5*, 106.
5. Kreider, M.L.; Panko, J.M.; McAtee, B.L.; Sweet, L.I.; Finley, B.L. Physical and chemical characterization of tire-related particles: Comparison of particles generated using different methodologies. *Sci. Total Environ.* **2010**, *408*, 652–659. [[CrossRef](#)] [[PubMed](#)]
6. Kupiainen, K.J.; Tervahattu, H.; Raisanen, M.; Makela, T.; Aurela, M.; Hillamo, R. Size and composition of airborne particles from pavement wear, tires, and traction sanding. *Environ. Sci. Technol.* **2005**, *39*, 699–706. [[CrossRef](#)] [[PubMed](#)]
7. Hildemann, L.M.; Markowski, G.R.; Cass, G.R. Chemical composition of emissions from urban sources of fine organic aerosol. *Environ. Sci. Technol.* **1991**, *25*, 744–759. [[CrossRef](#)]
8. Gustafsson, M.; Blomqvist, G.; Gudmundsson, A.; Dahl, A.; Swietlicki, E.; Bohgard, M.; Lindbom, J.; Ljungman, A. Properties and toxicological effects of particles from the interaction between tires, road pavement and winter traction material. *Sci. Total Environ.* **2008**, *393*, 226–240. [[CrossRef](#)] [[PubMed](#)]

9. Dahl, A.; Gharibi, A.; Swietlicki, E.; Gudmundsson, A.; Bohgard, M.; Ljungman, A.; Blomqvist, G.; Gustafsson, M. Traffic-generated emissions of ultrafine particles from pavement–tire interface. *Atmos. Environ.* **2006**, *40*, 1314–1323. [[CrossRef](#)]
10. Pant, P.; Harrison, R.M. Estimation of the contribution of road traffic emissions to particulate matter concentrations from field measurements: A review. *Atmos. Environ.* **2013**, *77*, 78–97. [[CrossRef](#)]
11. Harrison, R.M.; Jones, A.M.; Gietl, J.; Yin, J.; Green, D.C. Estimation of the contributions of brake dust, tire wear, and resuspension to non-exhaust traffic particles derived from atmospheric measurements. *Environ. Sci. Technol.* **2012**, *46*, 6523–6529. [[CrossRef](#)] [[PubMed](#)]
12. Beji, A.; Deboudt, K.; Muresan, B.; Khardi, S.; Flament, P.; Fourmentin, M.; Lumiere, L. Physical and chemical characteristics of particles emitted by a passenger vehicle at the tire-road contact. *Chemosphere* **2023**, *340*, 139874. [[CrossRef](#)] [[PubMed](#)]
13. Feng, X.L.; Shao, L.Y.; Xi, C.X.; Jones, T.P.; Zhang, D.Z.; BéruBé, K.A. Particle-induced oxidative damage by indoor size-segregated particulate matter from coal-burning homes in the Xuanwei lung cancer epidemic area, Yunnan Province, China. *Chemosphere* **2020**, *256*, 127058. [[CrossRef](#)]
14. Sadiq, A.A.; Khardi, S.; Lazar, A.N.; Bello, I.W.; Salam, S.P.; Faruk, A.; Alao, M.A.; Catinon, M.; Vincent, M.; Trunfio-Sfarghiu, A.M. A Characterization and Cell Toxicity Assessment of Particulate Pollutants from Road Traffic Sites in Kano State, Nigeria. *Atmosphere* **2022**, *13*, 655. [[CrossRef](#)]
15. Londahl, J.; Pagels, J.; Swietlicki, E.; Zhou, J.C.; Ketzler, M.; Massling, A.; Bohgard, M. A set-up for field studies of respiratory tract deposition of fine and ultrafine particles in humans. *J. Aerosol. Sci.* **2006**, *37*, 1152–1163. [[CrossRef](#)]
16. Poma, A.; Vecchiotti, G.; Colafarina, S.; Zarivi, O.; Arrizza, L.; Di Carlo, P.; Di Cola, A. Particle debris generated from passenger and truck tires induces different genotoxicity and inflammatory responses in the RAW 264.7 cell line. *Nanomaterials* **2023**, *13*, 756. [[CrossRef](#)] [[PubMed](#)]
17. Mantecca, P.; Farina, F.; Moschini, E.; Gallinotti, D.; Gualtieri, M.; Rohr, A.; Sancini, G.; Palestini, P.; Camatini, M. Comparative acute lung inflammation induced by atmospheric PM and size-fractionated tire particles. *Toxicol. Lett.* **2010**, *198*, 244–254. [[CrossRef](#)]
18. Kreider, M.L.; Unice, K.U.; Panko, J.M. Human health risk assessment of Tire and Road Wear Particles (TRWP) in air. *Hum. Ecol. Risk Assess. Int. J.* **2020**, *26*, 2567–2585. [[CrossRef](#)]
19. Statistica. *Trafic Moyen Quotidien sur le Réseau Autoroutier en France de 2012 à 2018, Selon le Type de Véhicule*; Statistica: Paris, France, 2021.
20. Tibidibito. 2022. Available online: <https://commons.wikimedia.org> (accessed on 1 January 2024).
21. Altimetry of Lyon. 2023. Available online: <https://fr.lyonmap360.com/plan-topographique-lyon> (accessed on 1 January 2024).
22. GRIMM Aerosol Technik (Grimm Group). 2021. Available online: <https://www.durag.com/en/grimm-aerosol-technik> (accessed on 1 January 2024).
23. Duma, Z.S.; Sihvonen, T.; Havukainen, J.; Reinikainen, V.; Reinikainen, S.P. Optimizing energy dispersive X-Ray Spectroscopy (EDS) image fusion to Scanning Electron Microscopy (SEM) images. *Micron* **2022**, *163*, 103361. [[CrossRef](#)]
24. JEOL Ltd. Available online: <https://www.jeol.com/products/scientific/sem/JSM-6510series.php> (accessed on 1 January 2024).
25. Rahim, M.; Ragavan, M.; Deja, S.; Merritt, M.E.; Burgess, S.C.; Young, J.D. INCA 2.0: A tool for integrated, dynamic modeling of NMR- and MS-based isotopomer measurements and rigorous metabolic flux analysis. *Metab. Eng.* **2022**, *69*, 275–285. [[CrossRef](#)]
26. Van Cutsem, B. *Classification and Dissimilarity Analysis*; Lecture Notes in Statistics; Springer: New York, NY, USA, 1994; ISBN 0-387-94400-1.
27. Cura, R.; Vaudor, L. Manipulation de Données Avec R 1—Fondamentaux. D’après L. Vaudor: Formation startR. École Thématique GeoViz. 2018.
28. Romesburg, C. *Cluster Analysis for Researchers*; Lulu Press: Morrisville, NC, USA, 2004.
29. Fernández, C.; Steel, M.F. Multivariate Student-t regression models: Pitfalls and inference. *Biometrika* **1999**, *86*, 153–167. [[CrossRef](#)]
30. Muirhead, R.J. *Aspects of Multivariate Statistical Theory*; Wiley: Hoboken, NJ, USA, 2009.
31. Li, H.; Qin, Q.; Jones, G.L. Convergence analysis of data augmentation algorithms for Bayesian robust multivariate linear regression with incomplete data. *J. Multivar. Anal.* **2024**, *202*, 105296. [[CrossRef](#)]
32. Husson, F.; Josse, J.; Le, S.; Mazet, J. *Multivariate Exploratory Data Analysis and Data Mining, Version 2.4*; Package ‘FactoMineR’; The R Project for Statistical Computing: Vienna, Austria, 2020.
33. Piscitello, A.; Bianco, C.; Casasso, A.; Sethi, R. Non-exhaust traffic emissions: Sources, characterization, and mitigation measures. *Sci. Total Environ.* **2021**, *766*, 144440. [[CrossRef](#)] [[PubMed](#)]
34. Moreno-Ríos, A.L.; Tejada-Benítez, L.P.; Bustillo-Lecompte, C.F. Sources, characteristics, toxicity, and control of ultrafine particles: An overview. *Geosci. Front.* **2022**, *13*, 101147. [[CrossRef](#)]
35. Alves, C.A.; Vicente, A.M.P.; Calvo, A.I.; Baumgardner, D.; Amato, F.; Querol, X.; Pio, C.; Gustafsson, M. Physical and chemical properties of non-exhaust particles generated from wear between pavements and tyres. *Atmos. Environ.* **2020**, *224*, 117252. [[CrossRef](#)]
36. Zhang, Q.; Fang, T.; Men, Z.; Wei, N.; Peng, J.; Du, T.; Zhang, X.; Ma, Y.; Wu, L.; Mao, H. Direct measurement of brake and tire wear particles based on real-world driving conditions. *Sci. Total Environ.* **2024**, *906*, 167764. [[CrossRef](#)] [[PubMed](#)]

37. Zhang, L.; Wang, L. Optimization of site investigation program for reliability assessment of undrained slope using Spearman rank correlation coefficient. *Comput. Geotech.* **2023**, *155*, 105208. [[CrossRef](#)]
38. Aatmeeyata; Kaul, D.S.; Sharma, M. Traffic generated non-exhaust particulate emissions from concrete pavement: A mass and particle size study for two-wheelers and small cars. *Atmos. Environ.* **2009**, *43*, 5691–5697. [[CrossRef](#)]

Disclaimer/Publisher’s Note: The statements, opinions and data contained in all publications are solely those of the individual author(s) and contributor(s) and not of MDPI and/or the editor(s). MDPI and/or the editor(s) disclaim responsibility for any injury to people or property resulting from any ideas, methods, instructions or products referred to in the content.